Synthesis and Characterization of Highly Branched Poly(*p*-phenylenevinylene) Derivatives for Polymer Light-Emitting Diode Applications

Jin Su Park, Myungkwan Song, Kyung-Jin Yoon, In Ae Shin, Myung Jin Lee, Tae In Ryu, and Sung-Ho Jin*

Department of Chemistry Education and Interdisciplinary Program of Advanced Information and Display Materials, Pusan National University, Busan 609-735, Korea

Yeong-Soon Gal

Polymer Chemistry Laboratory, Kyungil University, Hayang 712-701, Korea

Jae Wook Lee

Department of Chemistry, Dong-A University, Busan 604-714, Korea

Received April 12, 2008; Revised Manuscript Received June 12, 2008

ABSTRACT: A new series of green electroluminescence polymers, poly[{2-(3,7-dimethyloctyloxy)-3,5,6-trimethoxy-1,4-phenylenevinylene}] [poly($3OC_1OC_{10}$-PV)] and poly[2-(3-dimethyldodecylsilylphenyl)-1,4-phenylenevinylene] [poly(*m*-SiPh-PV)], and their corresponding copolymers, poly[2-{(3,7-dimethyloctyloxy)-3,5,6-trimethoxy-1,4-phenylenevinylene}-*co*-(2-(3-dimethyldodecylsilylphenyl)-1,4-phenylenevinylene)] [poly($3OC_1OC_{10}$-PV-*co*-*m*-SiPh-PV)], were synthesized through the Gilch polymerization method. The newly designed and highly branched molecular structures of the polymers, poly($3OC_1OC_{10}$-PV), poly($3OC_1OC_{10}$-PV-*co*-*m*-SiPh-PV) and poly(*m*-SiPh-PV), were completely soluble in common organic solvents and easily spin-coated onto an ITO-coated glass substrate to obtain high quality optical thin films. The weight-average molecular weight (M_w) and polydispersity of poly($3OC_1OC_{10}$-PV) were 17.3×10^4 and 2.9, respectively, while those of poly($3OC_1OC_{10}$-PV-*co*-*m*-SiPh-PV) were in the range of $(20.5-101.8) \times 10^4$ and 3.2−6.7, respectively. We fabricated polymer light-emitting diodes in ITO/PEDOT/emitting polymer/cathode configurations using either double-layer, LiF/Al, or triple-layer, LiF/Ca/Al, cathode structures. The emission maxima of the polymers, regardless of the copolymer compositions, were around 544−560 nm, which is a green color. The turn-on voltages of the EL polymers were in the range of 2.5−5.5 V, and the maximum brightness and luminance efficiency were 15,330 cd/m^2 at 10 V and 4.44 cd/A at 11 V, respectively.

Introduction

Since the work of Friend's group on electroluminescence (EL) of π-conjugated polymers, research around the world has expanded in order to develop new display technologies.[1] Polymer light-emitting diodes (PLEDs) present many attractive properties, such as low driving voltage, wide color range, low cost, flexibility, and easy processing. For practical application of PLEDs, high quantum efficiencies combined with long lifetimes are crucial for passive and active driving displays. PLED performance is closely dependent on the charge balance between holes and electrons which are injected respectively from the anode and the cathode. Many research groups have proposed various techniques for improving device performance such as the use of a phosphorescence emitter,[2] controlling the conjugation length,[3] blending with small organic molecules,[4] changing the polymer structures to form asymmetric poly(*p*-phenylenevinylene) (PPV) derivatives,[5] and using an electron-transporting layer.[6] Moreover, the major approach has been the energy barrier modulation of the electron injection contacts, which can be obtained by various methods, including the modification of the device structure by introducing an electron injection and transport layer and the use of low work function metals as a cathode.[7,8] The use of a metal with a low work function such as calcium, magnesium, or lithium as the cathode can lower the charge injection barrier at the cathode and improve the luminance efficiency by balancing the injection rates of electrons and holes. However, these metals have high chemical reactivity with respect to oxygen and moisture, which limits their practical use. In order to achieve high performance of PLEDs, devices were fabricated with a low work function cathode with a 200 nm Al film being deposited subsequently onto the low work function cathode.

Among the π-conjugated polymers, PPV derivatives have attracted a great deal of attention because of their potential application as EL materials for PLEDs.[9] PPV-based EL polymers have many advantages such as high photoluminescence (PL) and EL efficiencies, thermal, and chemical stabilities, and the ability to tune the emission colors by controlling the coplanarity or copolymer system. Recently, various bulky substituents such as dimethyldodecylsilylphenyl, alkylsilyl, phenyl, and fluorenyl groups have been substituted in the PPV backbone to suppress the intermolecular interactions leading to the formation of excimers.[5,10−15] The design and synthesis of thermally stable new materials and charge transport polymers are needed for improving their PLED performance and durability. The copolymerization process has been used widely in the preparation of EL polymers with the aim of achieving a low turn-on voltage, high brightness, high luminance efficiency, and easy tuning of the emission colors as a result of the energy transfer that arises from synergistic effects between the two monomers.[13] In our research in this area, we have previously reported novel EL polymers such as alkyloxyphenoxy and 1,3,4-oxadiazole-substituted PPVs, the blending of systems with 1,3,4-

* Corresponding author. Tel: +82-51-510-2727. Fax: +82-51-581-2348. E-mail: shjin@pusan.ac.kr.

10.1021/ma8008178 CCC: $40.75
Published on Web 08/29/2008

oxadiazole containing electron transfer polymers, the synthesis of alternating copolymers composed of PPV segments and aromatic amine blocks, and poly(9,9-dioctylfluorenyl-2,7-vinylene) and its copolymers with MEH-PPV segments and highly luminescent poly(*m*-SiPh-PV) derivatives.[5,16−21] Recently, we reported poly(PDOT-PV) and statistical copolymers poly(PDOT-PV-*co*-*m*-SiPh-PV) with turn-on voltages in the range of 6.0−9.0 V and a maximum brightness of 5,127 cd/m^2 at 18 V.[22]

As an extension of our work, in this article, we design a new series of EL polymers with poly($3OC_1OC_{10}$-PV) containing three methoxy and 3,7-dimethyloctyloxy substituents and its copolymers with poly(*m*-SiPh-PV) segments. The addition of the methoxy and 3,7-dimethyloctyloxy groups in the main chain is expected to tune the highest occupied molecular orbital (HOMO) level of EL polymers as well as suppress the excimer formation due to intermolecular interaction. We describe their thermal, optical, and electrochemical properties as well as EL properties.

Experimental Section

Synthesis of 2,4,5-Trimethoxyphenol (1).[23] To a solution of 2,4,5-trimethoxybenzaldehyde (10 g, 51 mmol) in dry CH_2Cl_2 (170 mL), mCPBA (77%, 13.7 g, 61 mmol) was added at 0 °C. The mixture was stirred at room temperature for 12 h, and the resulting precipitates were filtered off. The filtrate was washed with saturated $NaHCO_3$ solution and brine. The organic layer was dried and concentrated and then hydrolyzed with 10% KOH in EtOH at 50 °C for 2 h. The mixture was extracted with ether, and the aqueous layer was acidified with dilute HCl and again extracted with CH_2Cl_2. The organic layer was washed with brine, dried over $MgSO_4$, and concentrated. The residue was subjected to a column chromatography using hexane:ethyl acetate (4:1) as an eluent to give 2,4,5-trimethoxyphenol (**1**) as a light pink solid (7 g, 75%). ^{1}H NMR (300 MHz, $CDCl_3$): δ (ppm) 3.825 (s, 3H), 3.847 (s, 3H), 3.864 (s, 3H), 5.28 (s, 1H), 6.58 (S, 1H), 6.61 (s, 1H). ^{13}C NMR (300 MHz, $CDCl_3$): δ (ppm) 143.24, 141.51, 139.37, 139.23, 100.81, 99.61, 56.52, 56.23, 55.73. Anal. Calcd for $C_9H_{12}O_4$: C, 58.69; H, 6.57; O, 34.75. Found: C, 58.20; H, 6.79; O, 35.02.

Synthesis of 1-(3,7-dimethyloctyloxy)-2,4,5-trimethoxybenzene (2). 2,4,5-Trimethoxyphenol (7 g, 38 mmol), K_2CO_3 (16.4 g, 119 mmol) and a catalytic amount of KI was dissolved in DMF (100 mL), and then 3,7-dimethyloctyl bromide (17.5 g, 79 mmol) was added dropwise and stirred at 50 °C for 12 h. The mixture was added to water (100 mL), and then 10% NaOH (100 mL) solution was added and stirred for 10 min. The mixture was extracted with water and *n*-hexane several times. The combined organic layers were dried over anhydrous $MgSO_4$ and filtered. The solvent was removed by evaporation under reduced pressure. The oil residue was purified by column chromatography on silica gel using *n*-hexane as an eluent to give 1-(3,7-dimethyloctyloxy)-2,4,5-trimethoxybenzene (**2**) (6.95 g, 56%). ^{1}H NMR (300 MHz, $CDCl_3$): δ (ppm) 0.867 (d, J = 6.6 Hz, 6H), 0.945 (d, J = 6.3 Hz, 3H), 1.12−1.38 (m, 6H), 1.48−1.74 (m, 3H), 1.80−1.91 (m, 1H), 3.834 (s, 3H), 3.839 (s, 3H), 3.847 (s, 3H), 3.96−4.04 (m, 2H), 6.59 (s, 1H), 6.61 (s, 1H). ^{13}C NMR (300 MHz, $CDCl_3$): δ (ppm) 143.43, 142.98, 142.78, 142.18, 102.59, 100.96, 68.25, 56.50, 56.05, 38.59, 36.65, 35.91, 29.11, 27.27, 24.01, 22.00, 21.91, 18.99. Anal. Calcd for $C_{19}H_{11}O_4$: C, 75.24; H, 3.66; O, 21.10. Found: C, 75.22; H, 3.83; O, 20.11.

Synthesis of 2-(3,7-dimethyloctyloxy)-1,4-bis(chloromethyl)-3,5,6-trimethoxybenzene (3). 1-(3,7-Dimethyloctyloxy)-2,4,5-trimethoxybenzene (6.95 g, 21.4 mmol) and chloromethyl methyl ether (8.62 g, 107 mmol) were added to H_2SO_4 (1.38 mL). The mixture was stirred at 50 °C for 10 h. Then the reaction mixture was extracted with water and *n*-hexane several times. The combined organic layers were dried over anhydrous $MgSO_4$ and filtered. The solvent was removed by evaporation under reduced pressure. The oil residue was purified by column chromatography on silica gel using *n*-hexane:toluene (10:1) as an eluent to give 2-(3,7-dimethyloctyloxy)-1,4-bis(chloromethyl)-3,5,6-trimethoxybenzene (**3**) (1.89 g, 21%). ^{1}H NMR (300 MHz, $CDCl_3$): δ (ppm) 0.887 (d, J = 6.6 Hz, 6H), 0.978 (d, J = 6.3 Hz, 3H), 1.14−1.42 (m, 6H), 1.50−1.78 (m, 3H), 1.83−1.94 (m, 1H), 3.931 (s, 3H), 3.942 (s, 3H), 3.946 (s, 3H), 4.07−4.14 (t, J = 7.5 Hz, 2H), 4.69 (s, 4H). ^{13}C NMR (300 MHz, $CDCl_3$): δ (ppm) 147.82, 147.53, 147.11, 127.07, 126.93, 72.32, 61.14, 60.94, 39.20, 37.31, 37.24, 35.34, 35.27, 29.68, 27.88, 24.60, 22.61, 22.51, 19.65. Anal. Calcd for $C_{21}H_{13}Cl_2O_4$: C, 59.85; H, 8.13; Cl, 16.83; O, 15.19. Found: C, 60.03; H, 8.38; O, 15.35.

Synthesis of Poly[2-{(3,7-dimethyloctyloxy)-3,5,6-trimethoxy-1,4-phenylenevinylene}-*co*-(2-(3-dimethyldodecylsilylphenyl)-1,4-phenylenevinylene)] [Poly($3OC_1OC_{10}$-PV-*co*-*m*-SiPh-PV)] (44:56 mol %). A solution of potassium *tert*-butoxide (1.0 M THF solution, 4.3 mL) was added over 30 min using a syringe pump to a stirred solution of 2-(3,7-dimethyloctyloxy)-1,4-bis(chloromethyl)-3,5,6-trimethoxybenzene (**3**) (0.152 g, 0.36 mmol) and 1,4-bis(bromomethyl)-2-(3-dimethyldodecylsilylphenyl)benzene (**4**) (0.205 g, 0.36 mmol) in dry THF (20 mL) at 0 °C. The reaction mixture was stirred at room temperature for 1 h and exhibited gradually increasing viscosity and green fluorescence during that period. The polymer was sequentially end-capped with a small amount of 4-*tert*-butylbenzyl bromide and further stirred for 1 h. The polymerization solution was poured into methanol (500 mL), and the crude polymer was successively Soxhlet extracted with methanol, isopropyl alcohol and acetone to remove the unreacted monomers, impurities and oligomers. After carrying out the normal polymer purification procedures described above, the solution of the polymer in chloroform was dialyzed against chloroform solvent for 5 days while stirring to remove the medium molecular weight (MWCO 80,000) polymer portions. After dialysis, the purified fibrous EL polymer was obtained by pouring the solution into methanol (500 mL), which was then filtered and vaccuum-dried to give a bright green polymer fiber, poly($3OC_1OC_{10}$-PV-*co*-*m*-SiPh-PV) (44:56) (0.12 g, 46%). ^{1}H NMR (500 MHz, $CDCl_3$): δ (ppm) 8.0−7.0 (br, 12H, aromatic protons and vinylic protons), 4.3−3.5 (br, 11H, methoxy protons and methylene protons next to oxygen), 2.1−0.7 (br, 55H, aliphatic protons), 0.4−0.2 (br, 7.5H, $Si(CH_3)_2$). Anal. Calcd for $(C_{56}H_{82}O_4Si)_n$: C, 79.38; H, 9.75; O, 7.55; Si, 3.31. Found: C, 79.69; H, 9.80; O, 7.22.

The homopolymer, poly[{2-(3,7-dimethyloctyloxy)-3,5,6-trimethoxy-1,4-phenylenevinylene}] [poly($3OC_1OC_{10}$-PV)], poly[2-(3-dimethyldodecylsilylphenyl)-1,4-phenylenevinylene] [poly(*m*-SiPh-PV)], and the copolymers, poly($3OC_1OC_{10}$PV-*co*-*m*-SiPh-PV) of 2-(3,7-dimethyloctyloxy)-1,4-bis(chloromethyl)-3,5,6-trimethoxybenzene (**3**) and 1,4-bis(bromomethyl)-2-(3-dimethyldodecylsilylphenyl)benzene (**4**) were synthesized with various feed ratios using a method similar to that of poly($3OC_1OC_{10}$-PV-*co*-*m*-SiPh-PV) (44:56). The composition ratios of the copolymers were calculated from the integration ratios of the 3.5−4.3 ppm and 0.2−0.4 ppm peaks in the ^{1}H NMR spectrum.

Poly($3OC_1OC_{10}$-PV). ^{1}H NMR (500 MHz, $CDCl_3$): δ (ppm) 8.0−7.6 (br, 2H, vinylic protons), 4.3−3.5 (br, 11H, methoxy protons and methylene protons next to oxygen), 2.13−0.74 (br, 19H, aliphatic protons). Anal. Calcd for $C_{21}H_{32}O_4$: C, 72.38; H, 9.26; O, 18.36. Found: C, 72.35; H, 9.66; O, 17.62.

Poly($3OC_1OC_{10}$-PV-*co*-*m*-SiPh-PV) (93:7 mol %). Anal. Calcd for $(C_{56}H_{82}O_4Si)_n$: C,72.98; H, 9.12; O, 17.31; Si, 0.58. Found: C, 73.02; H, 9.03; O, 17.71.

Poly($3OC_1OC_{10}$-PV-*co*-*m*-SiPh-PV) (76:24 mol %). ^{1}H NMR (500 MHz, $CDCl_3$): δ (ppm) 8.0−7.0 (br, 20H, aromatic protons and vinylic protons), 4.3−3.5 (br, 11H, methoxy protons and methylene protons next to oxygen), 2.1−0.7 (br, 73H, aliphatic protons), 0.4−0.2 (br, 6H, $Si(CH_3)_2$). Anal. Calcd for $(C_{56}H_{82}O_4Si)_n$: C, 75.37; H, 9.62; O, 13.09; Si, 1.92. Found: C, 76.44; H, 7.99; O, 13.25.

Poly($3OC_1OC_{10}$-PV-*co*-*m*-SiPh-PV) (6:94 mol %). Anal. Calcd for $(C_{56}H_{82}O_4Si)_n$: C, 82.49; H, 9.94; O, 1.0; Si, 6.58. Found: C, 82.06; H, 10.54; O, 0.86.

Scheme 1

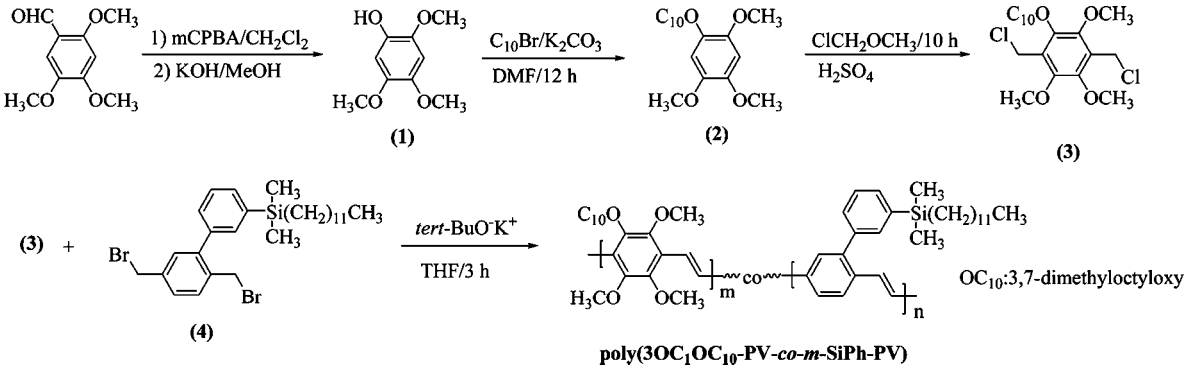

Table 1. Polymerization Results and Thermal Properties of Poly(3OC$_1$OC$_{10}$-PV), Poly(3OC$_1$OC$_{10}$-PV-*co*-*m*-SiPh-PV) and Poly(*m*-SiPh-PV)

polymer	M_w[a] (10^4)	PDI[a]	yield (%)	DSC[b]	TGA[c]
poly(3OC$_1$OC$_{10}$-PV)	17.3	2.9	38	100	358
poly(3OC1OC10-PV-*co*-*m*-SiPh-PV) (93:7)[d]	20.5	4.5	48	100	358
poly(3OC1OC10-PV-*co*-*m*-SiPh-PV) (76:24)	101.8	3.2	51	110	363
poly(3OC1OC10-PV-*co*-*m*-SiPh-PV) (44:56)	58.8	6.7	46	120	373
poly(3OC1OC10-PV-*co*-*m*-SiPh-PV) (6:94)	136.4	6.4	47	132	396
poly(*m*-SiPh-PV)	25.6	5.4	62	154	408

[a] M_w and PDI of the polymers were determined by GPC using polystyrene standards. [b] Determined by DSC at a heating rate of 10 °C /min under N_2 atmosphere. [c] TGA was measured at temperature of 5% weight loss for the polymers. [d] Calculated from ^{1}H NMR.

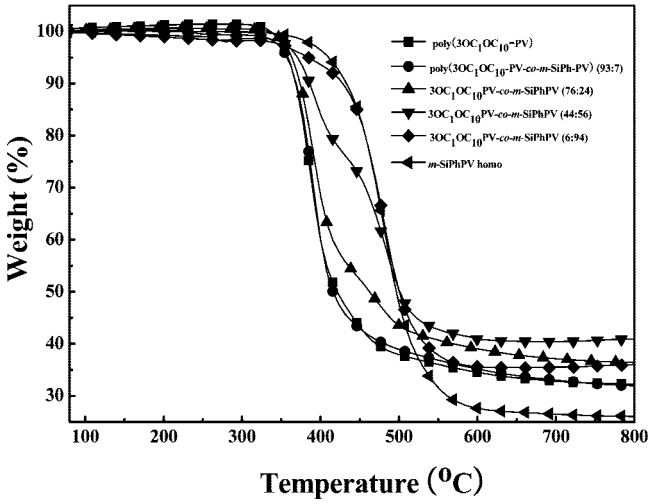

Figure 1. TGA thermogram of poly(3OC$_1$OC$_{10}$-PV), poly(3OC$_1$OC$_{10}$-PV-*co*-*m*-SiPh-PV) and poly(*m*-SiPh-PV).

Poly(*m*-SiPh-PV). ^{1}H NMR ($CDCl_3$): δ (ppm) 7.80−7.10 (br, 9H, aromatic protons and vinylic protons) 1.52−1.10 (m, 22H, aliphatic protons) 0.98−0.70 (m, 5H, $SiCH_2$ and methyl protons) 0.30 (s, 6H, methylene protons and next to silicon). Anal. Calcd for $C_{28}H_{41}Si$: C, 82.69; H, 9.96; Si, 6.91; Found: C, 82.90; H, 9.86.

Materials, Measurements, and Instruments. 2,4,5-Trimethoxybenzaldehyde, *m*-chloroperoxybenzoic acid (77%), chloromethyl methyl ether, 1,3-dibromobenzene, chlorododecyldimethylsilane, 2-bromo-*p*-xylene, *n*-butyllithium (1.6 M hexane solution), 1,3-[bis(diphenylphosphino)propane]dichloronickel(II) [$NiCl_2$(dppp)], magnesium granules, *N*-bromosuccinimide (NBS), potassium *tert*-butoxide (1.0 M solution in THF), LiF, Ca, and Al were purchased from Aldrich Co. and used without further purification unless otherwise noted. Solvents were dried and purified by fractional distillation over sodium/benzophenone and handled in a moisture free atmosphere. Column chromatography was performed using silica gel (Merck, 250−430 mesh). The polyvinylidene fluoride dialysis membrane was purchased from Spectrum Co. ^{1}H and ^{13}C NMR spectra were recorded on a Bruker AM-300 or Inova-500 (500 MHz) spectrometer, and chemical shifts were recorded in ppm units with chloroform as an internal standard. UV−visible and emission spectra were recorded with a Shimadzu UV-3100 and Hitachi F-4500 fluorescence spectrophotometers. Solid-state emission measurements were carried out by supporting each film on a quartz substrate that was mounted to receive front-face excitation at an angle of less than 45°. Each polymer film was excited with several portions of visible light from a xenon lamp. The molecular weight and polydispersity of the polymer were determined by gel permeation chromatography (GPC) using a PLgel 5 μm MIXED-C column on an Agilent 1100 series liquid chromatography system with THF as an eluent and calibration with polystyrene standards. Thermal analyses were carried out on a Mettler Toledo TGA/SDTA 851, DSC 822 analyzer under N_2 atmosphere at a heating rate of 10 °C/min. Cyclic voltammetry (CV) was carried out with a Bioanalytical Systems CV-50W voltammetric analyzer at a potential scan rate of 100−150 mV/s in 0.1 M solution of tetrabutylammonium tetrafluoroborate (Bu_4NBF_4) in anhydrous acetonitrile. Each polymer film was coated on a Pt disk electrode (0.2 cm^2) by spinning the electrode from the polymer solution (10 mg/mL). A platinum wire was used as the counter electrode, and an $Ag/AgNO_3$ electrode was used as the reference electrode. All of the electrochemical experiments were performed in a glovebox under an Ar atmosphere at room temperature. To measure EL properties, the PLED was constructed as follows. Each glass substrate was coated with a transparent ITO electrode (80 nm thick, 20 Ω/sq sheet resistance), washed thoroughly in acetone, isopropyl alcohol, and distilled water, dried under N_2 gas, heat dried, and finally treated with UV-ozone. The polymer films were prepared through spin-casting of polymer solution in concentration of 0.1 wt % in *o*-dichlorobenzene. Uniform and pinhole free films with thicknesses of approximately 80−100 nm were coated on a 40 nm layer of PEDOT:PSS layer (Baytron P Al 4083) on the ITO substrate used as the hole injection and transport layer. The film thickness was measured with an α-Step IQ surface profiler (KLA Tencor, San Jose, CA). LiF, Ca, and Al metal were deposited on top of each polymer film through a mask by vacuum evaporation at a pressure below 10^{-6} Torr, yielding an active area of 4 mm^2. To characterize the device, the current density−voltage−luminescence (*J*−*V*−*L*) changes were measured using a current/voltage source meter (Keithley 238) and an optical power meter (CS-1000, LS-100). All processes and measurements mentioned above were carried out in the open air at room temperature.

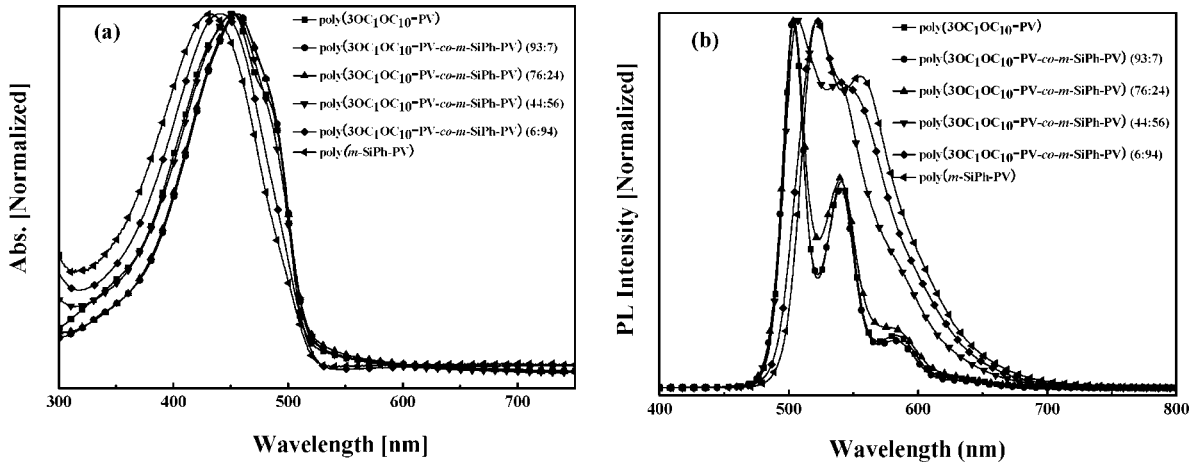

Figure 2. UV−visible absorption (a) and PL spectra (b) of poly($3OC_1OC_{10}$-PV), poly($3OC_1OC_{10}$-PV-*co*-*m*-SiPh-PV) and poly(*m*-SiPh-PV) in the solid state.

Table 2. Optical Properties of Poly($3OC_1OC_{10}$-PV), Poly($3OC_1OC_{10}$-PV-*co*-*m*-SiPh-PV) and Poly(*m*-SiPh-PV)

polymer	abs (nm)[a]	PL (nm)[a]	EL (nm)[b]	E_g (eV)[c]	Φ_{PL}[d]
poly($3OC_1OC_{10}$-PV)	451	504, 540, 585	509, 544, 587	2.41	27
poly(3OC1OC10-PV-*co*-*m*-SiPh-PV) (93:7)	456	504, 540, 585	507, 545, 585	2.40	20
poly(3OC1OC10-PV-*co*-*m*-SiPh-PV) (76:24)	455	504, 540, 585	510, 544	2.39	17
poly(3OC1OC10-PV-*co*-*m*-SiPh-PV) (44:56)	452	507, 540	527, 549	2.39	15
poly(3OC1OC10-PV-*co*-*m*-SiPh-PV) (6:94)	440	522, 550	528, 554	2.37	10
poly(*m*-SiPh-PV)	433	522, 556	530, 560	2.38	35

[a] Measured in the thin film onto the carboglass substrate. [b] EL spectra were measured by LiF/Ca/Al cathode. [c] Band gap estimated from the onset wavelength of the optical absorption. [d] Estimated by using a thin film of $\sim 10^{-3}$ M 9,10-diphenylanthracene in PMMA as a standard (83%).

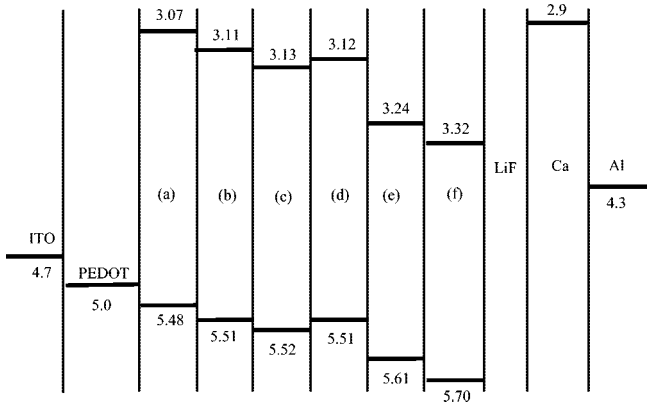

Figure 3. Energy band diagram of the ITO/PEDOT/light-emitting polymer/cathode devices, poly($3OC_1OC_{10}$-PV) (a), poly($3OC_1OC_{10}$-PV-*co*-*m*-SiPh-PV) (93:7) (b), poly($3OC_1OC_{10}$-PV-*co*-*m*-SiPh-PV) (76:24) (c), poly($3OC_1OC_{10}$-PV-*co*-*m*-SiPh-PV) (44:56) (d), poly($3OC_1OC_{10}$-PV-*co*-*m*-SiPh-PV) (6:94) (e), and poly(*m*-SiPh-PV) (f).

Results and Discussion

Synthesis and Characterization. The electronic and optical properties of π-conjugated polymers are governed by modifying the backbone's chemical structure. To adjust the HOMO and lowest unoccupied molecular orbital (LUMO) energy levels and the formation of amorphous morphology of the PPV-based EL polymers for improving the PLED performance, we first synthesized PPV-based homopolymer and copolymers containing the trimethoxy and 3,7-dimethyloctyloxy substituents into the polymer backbone via Gilch polymerization as shown in Scheme 1. 1-(3,7-Dimethyloctyloxy)-2,4,5-trimethoxybenzene (**2**), 2-(3,7-dimethyloctyloxy)-1,4-bis(chloromethyl)-3,5,6-trimethoxybenzene (**3**) and 1,4-bis(bromomethyl)-2-(3-dimethyldodecylsilylphenyl) benzene (**4**) were synthesized according to the reported literature.[5,23,24] Chloromethylation in the benzene ring with electron-donating alkyloxy substituents was easily obtained using fuming sulfuric acid and chloromethyl methyl ether at 0 °C to give a high conversion of chloromethylation. The homopolymerization of 2-(3,7-dimethyloctyloxy)-1,4-bis-(chloromethyl)-3,5,6-trimethoxybenzene (**3**) and copolymerization with 1,4-bis(bromomethyl)-2-(3-dimethyldodecylsilylphenyl)benzene (**4**) was performed with an excess of potassium *tert*-butoxide in THF at room temperature for 2.5 h under a N_2 atmosphere. The resulting EL polymers, poly($3OC_1OC_{10}$-PV), poly($3OC_1OC_{10}$-PV-*co*-*m*-SiPh-PV) and poly(*m*-SiPh-PV), were completely soluble in various organic solvents such as chloroform, chlorobenzene, toluene, xylene, THF. The molecular structures and thermal properties of the monomer and the polymers were identified by ^1H, ^{13}C NMR, elemental analysis, UV−vis spectra, DSC, and TGA thermograms. The disappearance of the characteristic chloromethyl proton peaks at around 4.69 ppm for monomers and the appearance of new vinylic proton peaks at 8.0−7.0 ppm with aromatic proton peaks in poly($3OC_1OC_{10}$-PV) and poly($3OC_1OC_{10}$-PV-*co*-*m*-SiPh-PV) confirmed the polymerization reaction. The copolymer compositions were calculated by comparing the peak area at 0.2−0.4 ppm of the dimethyl proton peak on the silcon atom and at 3.5−4.3 ppm of the methylene proton next to oxygen and the methoxy groups as side chains. Table 1 summarizes the polymerization results, molecular weights, and thermal characteristics of poly($3OC_1OC_{10}$-PV), poly($3OC_1OC_{10}$-PV-*co*-*m*-SiPh-PV) and poly(*m*-SiPh-PV) for comparison. Their weight-average molecular weight (M_w) and polydispersity of EL polymers were in the range of (17.3−136.4) × 10^4 and 2.95−6.70, respectively. The TGA results for EL polymer are shown in Figure 1. The polymers showed good thermal stability with a 5% weight loss over the temperature range of 358 to 408 °C under N_2 atmosphere. The glass transition temperatures (T_g) of poly($3OC_1OC_{10}$-PV) and poly($3OC_1OC_{10}$-PV-*co*-*m*-SiPh-PV) were in the range of 100 and 154 °C. These polymers had higher thermal stabilities than dialkyloxy-substituted PPVs or poly(9,9-dialkylfluorene)s.[25,26] The thermal stability of the polymers is adequate for the fabrication of PLED, and the T_g values indicate that the polymer should not deform or degrade

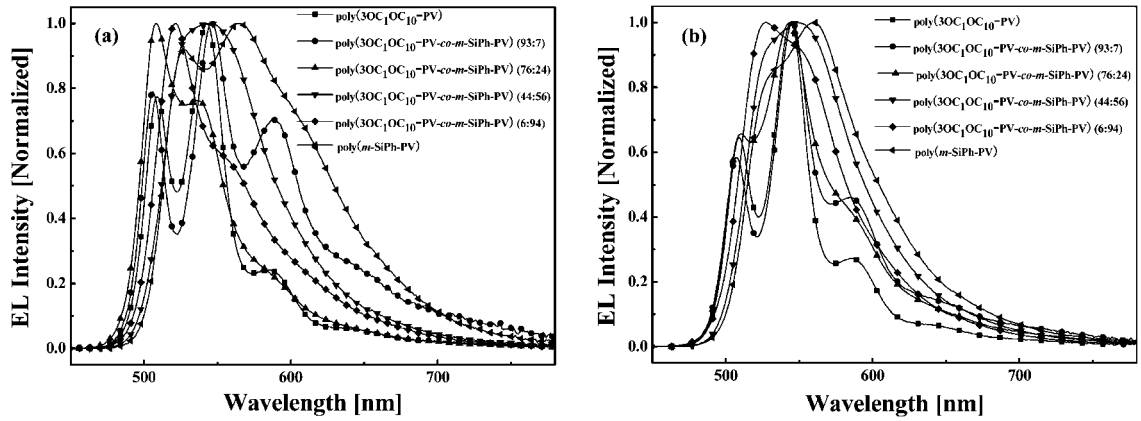

Figure 4. EL spectra of the ITO/PEDOT/light-emitting polymer/LiF/Al device (a) and the ITO/PEDOT/light-emitting polymer/LiF/Ca/Al device (b).

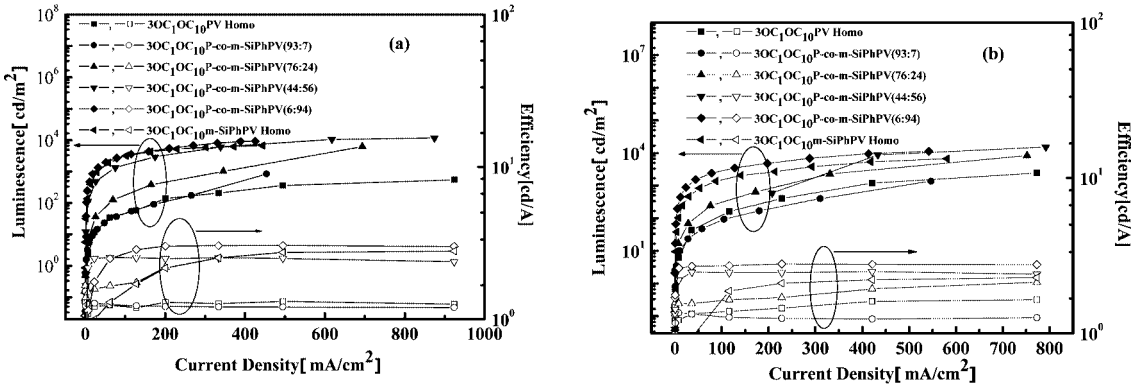

Figure 5. Current density−luminescence−current efficiency characteristic of the ITO/PEDOT/light emitting polymer/LiF/Al device (a) and the ITO/PEDOT/light-emitting polymer/LiF/Ca/Al device (b).

Table 3. PLED Performance of Poly($3OC_1OC_{10}$-PV), Poly($3OC_1OC_{10}$-PV-*co*-*m*-SiPh-PV) and Poly(*m*-SiPh-PV)

polymer	cathode	turn-on (V)	L_{max}[a] (cd/m^2, V)	LE_{max}[b] (cd/A, V)
poly($3OC_1OC_{10}$-PV)	LiF/Ca/Al	2.5	2249 (10)	0.32 (10)
	LiF/Al	2.7	550 (12)	0.19 (16)
poly(3OC1OC10-PV-*co*-*m*-SiPh-PV) (93:7)	LiF/Ca/Al	3.0	1360 (13)	0.25 (13)
	LiF/Al	3.0	847 (16)	0.19 (16)
poly(3OC1OC10-PV-*co*-*m*-SiPh-PV) (76:24)	LiF/Ca/Al	3.0	8209 (10)	1.09 (13)
	LiF/Al	3.0	6209 (9)	0.9 (9)
poly(3OC1OC10-PV-*co*-*m*-SiPh-PV) (44:56)	LiF/Ca/Al	3.0	15330 (10)	2.3 (9)
	LiF/Al	4.0	11720 (12)	1.84 (6)
poly(3OC1OC10-PV-*co*-*m*-SiPh-PV) (6:94)	LiF/Ca/Al	4.0	11170 (18)	3.98 (9)
	LiF/Al	4.0	9210 (21)	4.44 (11)
poly(*m*-SiPh-PV)	LiF/Ca/Al	4.0	5680 (18)	1.33 (17)
	LiF/Al	5.5	6370 (20)	3.27 (13)

[a] Maximum luminescence. [b] Maximum current efficiency.

in applied electric fields during the operation of EL devices.

Optical, Electrochemical, and Electroluminescent Properties of the Polymers. Figure 2 shows the optical absorption and PL spectra of poly($3OC_1OC_{10}$-PV), poly($3OC_1OC_{10}$-PV-*co*-*m*-SiPh-PV) and poly(*m*-SiPh-PV) thin films coated on a carbo-glass. The maximum absorption spectra of poly($3OC_1OC_{10}$-PV), poly($3OC_1OC_{10}$-PV-*co*-*m*-SiPh-PV) and poly(*m*-SiPh-PV) thin films exhibited a relatively sharp peak at around 456−433 nm due to the $\pi-\pi^*$ transition of the polymer backbone with an onset of absorption at 514, 518 and 521 nm, respectively. However, the slight red-shift of the poly($3OC_1OC_{10}$-PV-*co*-*m*-SiPh-PV) relative to that of poly(*m*-SiPh-PV) was probably due to the introduction of the poly($3OC_1OC_{10}$-PV) segment and the decreased torsional angle about the central ring due to the reduced steric hindrance of the dimethyldodecylsilylphenyl units. The absorption and emission maxima of polymers are summarized in Table 2, and the PL emission spectra in the thin film state are shown in Figure 2b. Notably, the PL spectra of poly($3OC_1OC_{10}$-PV) showed significantly more pronounced vibronic structures than those for the previously reported phenyl-substituted PPV derivative.[27] The PL emission spectrum of poly($3OC_1OC_{10}$-PV) shows three peaks centered at 504 nm as well as a weak shoulder centered at about 540 and 585 nm. As the poly(*m*-SiPh-PV) content in poly($3OC_1OC_{10}$-PV-*co*-*m*-SiPh-PV) was increased, the emission peaks were red-shifted from 504 to 522 nm and also the intensity of the shoulder peaks in the PL emission consistently increased. This may be due to the presence of an additional band that can be superimposed on the mutual PL band, which is observed as a more pronounced second vibronic band. Such an additional band feature might be due to the extended intermolecular interaction of the conjugated branches, as previously reported for many thiophene derivatives' pendant system.[28] No emission peak from poly($3OC_1OC_{10}$-PV) segments was observed, despite the presence of a 6

mol % of poly($3OC_1OC_{10}$-PV) in poly($3OC_1OC_{10}$-PV-*co*-*m*-SiPh-PV), which indicated that the efficient energy transfer occurred from the wide-band gap of poly($3OC_1OC_{10}$-PV) to the small-band gap of poly(*m*-SiPh-PV) segments.

The poly($3OC_1OC_{10}$-PV) and poly(*m*-SiPh-PV) thin films have a 27 and 35% of PL efficiency, respectively that is higher than that of poly($3OC_1OC_{10}$-PV-*co*-*m*-SiPh-PV). The PL efficiencies of the poly($3OC_1OC_{10}$-PV-*co*-*m*-SiPh-PV) copolymers with various poly(*m*-SiPh-PV) feed ratios are in the range 10−20%.

To investigate the charge carrier injection properties of the resulting EL polymers and evaluate their HOMO and LUMO energy levels, we carried out redox measurements using CV. The HOMO energies and band gaps were in the range of 5.48−5.70, and 2.37−2.41 eV, respectively for the EL polymers. The LUMO energy levels were calculated from the values of the band gaps and the HOMO energies. The energy band diagrams of EL polymers are displayed in Figure 3. The introduction of the electron-donating alkyloxy substituents into the PPV backbone decreased the oxidation potential compared to the introduction of dimethyldodecylsilylphenyl substituent into the PPV backbone, which increased the HOMO energy levels of poly($3OC_1OC_{10}$-PV) and poly($3OC_1OC_{10}$-PV-*co*-*m*-SiPh-PV) relative to that of poly(*m*-SiPh-PV). From Figure 3, the band offsets were 0.48−0.70 eV for hole injections at the interface of the PEDOT/HOMO state. The barrier heights of the EL polymers were found to be 0.98−1.23 eV at the interface of Al (4.3 eV)/LUMO state for electron injection indicating that the poly($3OC_1OC_{10}$-PV) segment facilitated the hole injection from the ITO electrodes. The energy band diagrams showed that the major carriers are the holes rather than the electrons due to the lower band offsets between the ITO and HOMO energy levels. These results coincided well with the *I*−*V* characteristics of the resulting EL polymers, which were determined by the majority carriers. The PLED efficiency is determined by the minority species injected through the higher of the barriers, which, in this case, is the electron. These energy band diagrams supported our prediction that the PLED performance of poly($3OC_1OC_{10}$-PV-*co*-*m*-SiPh-PV) (6:94) should be better than that of homopolymers and other copolymers because of the easy injection of holes and electrons from the electrodes in the PLEDs.

To evaluate the PLED performance, we fabricated multilayered PLEDs with two different cathode structures based on poly($3OC_1OC_{10}$-PV), poly($3OC_1OC_{10}$-PV-*co*-*m*-SiPh-PV) and poly(*m*-SiPh-PV) and compared them with ITO/PEDOT:PSS/emitting polymer/cathodes. The cathodes were either a bilayer of LiF (0.7 nm)/Al (200 nm) (cathode 1) or a triple layer of LiF (0.7 nm)/Ca (10 nm)/Al (200 nm) (cathode 2) for improved device performance.

Figure 4 shows the EL spectra of polymers for the cathode 1 and 2 devices. The EL spectra of the two types of PLEDs were almost identical to those of the PL spectra shown in Figure 2b and were slightly red-shifted with respect to the PL peaks of the thin films state. The red-shifted EL spectra were attributed to the injected current density, which extended the effective conjugation length. The maximum emission peak of poly($3OC_1OC_{10}$-PV) was at 544 nm with shoulder peaks at 509 and 587 nm. In addition, poly(*m*-SiPh-PV) exhibited bimodal peaks at 530 and 560 nm, which corresponded to a green color. The emission maximum of poly($3OC_1OC_{10}$-PV-*co*-*m*-SiPh-PV) was located between the maxima for the homopolymers.

Figure 5a shows the current density−luminescence−current efficiency characteristics of the EL polymers in the cathode 1 devices. The turn-on voltages of the bilayer cathode structure are between 2.7 and 5.5 V, and the PLED containing poly(*m*-SiPh-PV) had the highest turn-on voltage due to the high energy barrier or band offset between the ITO and HOMO states. The maximum brightness and current efficiency of EL polymers devices with the LiF/Al (cathode 1) were 11,720 cd/m^2 and 4.44 cd/A, respectively. To improve the PLED performance, the triple layer devices with LiF (0.7 nm)/Ca (10 nm)/Al (200 nm) (cathode 2) were fabricated. Figure 5b shows the current density−luminescence−current efficiency characteristics of the EL polymers in cathode 2 devices. The slight difference in the turn-on voltages of these two cathodes was attributed to the difference in the thickness of the spin-coated EL polymer films. The PLED performance of the cathode 2 devices was better than that of the cathode 1 devices, except for poly($3OC_1OC_{10}$-PV-*co*-*m*-SiPh-PV) (6:94) and poly(*m*-SiPh-PV), and the results are summarized in Table 3. The maximum brightness and current efficiency of the poly($3OC_1OC_{10}$-PV), poly($3OC_1OC_{10}$-PV-*co*-*m*-SiPh-PV) and poly(*m*-SiPh-PV) devices with cathode 2 were 15,530 cd/m^2 and 3.98 cd/A at 10 V, respectively. The improved electron transport due to the Ca layer in the cathode 2 devices reduced the electron accumulation and exciton quenching at the cathode and increased the efficiency of radiative carrier recombination.

Conclusions

This study focused on the molecular design and synthesis of highly branched PPV derivatives for PLED applications. The resulting EL polymers with high molecular weights were highly soluble in common organic solvents, which allowed them to be easily spin-coated onto glass substrates with high quality optical thin films. The introduction of the electron-donating alkyloxy substituents in the PPV's backbone decreased the HOMO binding energy and thus decreased PLEDs' turn-on voltage. We fabricated PLEDs in ITO/PEDOT/emitting polymer/cathode configurations with a cathode structure of either a bilayer of LiF/Al or a triple layer of LiF/Ca/Al cathode structure. The performance of PLEDs was higher with LiF/Ca/Al layer cathodes than with LiF/Al layer cathodes. The turn-on voltages were in the range of 2.5−5.5 V, and the maximum brightness and current efficiency were 15,330 cd/m^2 at 10 V and 4.44 cd/A at 11 V, respectively.

Acknowledgment. This work was supported by the Korea Science and Engineering Foundation (KOSEF) grant funded by the Korea government (MEST) (No. M10600000157-06J0000-15710).

References and Notes

(1) Burroughes, J. H.; Bradley, D. D. C.; Brown, A. R.; Marks, R. N.; Mackay, K.; Friend, R. H.; Burn, P. L.; Holmes, A. B. *Nature (London)* **1990**, *347*, 539.
(2) Schulz, G. L.; Chen, X.; Chen, S. A.; Holdcroft, S. *Macromolecules* **2006**, *39*, 9157.
(3) Padmanaban, G.; Ramakrishnan, S. *J. Am. Chem. Soc.* **2000**, *122*, 2244.
(4) Qu, J. Q.; Zhang, A. C.; Grimsdale, A. C.; Müllen, K.; Jaiser, F.; Yang, X. H.; Neher, D. *Macromolecules* **2004**, *37*, 8297.
(5) Jin, S. H.; Jang, M. S.; Suh, H. S. *Chem. Mater.* **2002**, *14*, 643.
(6) Wu, F. I.; Reddy, D. S.; Shu, C. F.; Liu, M. S.; Jen, A. K. Y. *Macromolecules* **2003**, *15*, 269.
(7) Hanson, E. L.; Guo, J.; Koch, N.; Schwartz, J.; Bernasek, S. L. *J. Am. Chem. Soc.* **2005**, *127*, 10058.
(8) Gong, X.; Moses, D.; Heeger, A. J.; Liu, S.; Jen, A. K. Y. *Appl. Phys. Lett.* **2003**, *83*, 183.
(9) Chuang, C. Y.; Shih, P. I.; Chien, C. H.; Wu, F. I.; Shu, C. F. *Macromolecules* **2007**, *40*, 247.
(10) Kim, S. T.; Hwang, D. H.; Li, X. C.; Gruner, J.; Holmes, A. B.; Friend, R. H.; Shim, H. K. *Adv. Mater.* **1996**, *8*, 979.
(11) Chen, Z. K.; Lee, N. H. S.; Huang, W.; Xu, Y. S.; Cao, Y. *Macromolecules* **2003**, *36*, 1009.
(12) Lee, S. H.; Jang, B. B.; Tsutsui, T. *Macromolecules* **2002**, *35*, 1356.
(13) Lu, J. L.; D'iotio, M.; Li, Y.; Ding, J.; Day, M. *Macromolecules* **2004**, *37*, 2442.
(14) Lam, J. W. Y.; Tang, B. Z. *J. Polym. Sci., Part A. Polym. Chem.* **2003**, *41*, 2607.
(15) Lam, J. W. Y.; Tang, B. Z. *Acc. Chem. Res.* **2005**, *38*, 745.

(16) Lee, J. H.; Yu, H. S.; Kim, W.; Gal, Y. S.; Park, J. H.; Jin, S. H. *J. Polym. Sci., Part A. Polym. Chem.* **2000**, *38*, 4185.
(17) Jin, S. H.; Kang, S. Y.; Yeom, I. S.; Kim, J. Y.; Park, S. H.; Lee, K. H.; Gal, Y. S.; Cho, H. N. *Chem. Mater.* **2002**, *14*, 5090.
(18) Jin, S. H.; Park, H. J.; Kim, J. Y.; Lee, K.; Lee, S. P.; Moon, D. K.; Lee, H. J.; Gal, Y. S. *Macromolecules* **2002**, *35*, 7532.
(19) Jin, S. H.; Kang, S. Y.; Kim, M. Y.; Yoon, U. C.; Kim, J. Y.; Lee, K. H.; Gal, Y. S. *Macromolecules* **2003**, *36*, 3841.
(20) Jin, S. H.; Kim, M. Y.; Kim, J. Y.; Lee, K.; Gal, Y. S. *J. Am. Chem. Soc.* **2004**, *126*, 2474.
(21) Jin, S. H.; Jung, H. H.; Hwang, C. K.; Koo, D. S.; Shin, W. S.; Kim, Y. I.; Lee, J. W.; Gal, Y. S. *J. Polym. Sci., Part A: Polym. Chem.* **2005**, *43*, 5062.
(22) Jeon, H. S.; Lee, S. K.; Lee, E. J.; Park, S. M.; Kim, S. C.; Jin, S. H.; Gal, Y. S.; Lee, J. W.; Im, C. *Macromolecules* **2007**, *40*, 4794.
(23) Stephane, P.; Michele, G.; Mohammad, S. *Tetrahedron* **1998**, *54*, 14791.
(24) Jin, S. H.; Jung, J. E.; Yeom, I. S.; Moon, S. B.; Koh, K.; Kim, S. H.; Gal, Y. S. *Eur. Polym. J.* **2002**, *38*, 895.
(25) Xia, C.; Advincula, R. C. *Macromolecules* **2001**, *34*, 5854.
(26) Kim, J. L.; Kim, J. K.; Cho, H. N.; Kim, D. Y.; Kim, C. Y.; Hong, S. I. *Macromolecules* **2000**, *33*, 5880.
(27) Im, C.; Lupton, J. M.; Schouwink, P.; Heun, S.; Becker, H.; Bässler, H. *J. Chem. Phys.* **2002**, *117*, 1395.
(28) Turbiez, M.; Frère, P.; Allain, M.; Gallego-Planas, N.; Roncali, J. *Macromolecules* **2005**, *38*, 6806.

MA8008178